Journal of Achievements in Materials and Manufacturing Engineering
VOLUME 33
ISSUE 2
April
2009

A modification of the method for determination of surface fractal dimension and multifractal analysis

W. Kwaśny*
Division of Materials Processing Technology, Management and Computer Techniques in Materials Science, Institute of Engineering Materials and Biomaterials, Silesian University of Technology, ul. Konarskiego 18a, 44-100 Gliwice, Poland
* Corresponding author: E-mail address: waldemar.kwasny@polsl.pl

Received 20.02.2009; published in revised form 01.04.2009

Methodology of research

ABSTRACT

Purpose: In this work modification of the PCM method for determination of the surface fractal dimension is proposed. Complete reasoning, leading to correct formula for determination $A_i(\delta)$ is presented. In order to test modified method, data sets characterised by fractional fractal dimension were generated.
Design/methodology/approach: Three different algorithms to receive data sets describing surfaces with fractional fractal dimension were exploited (two algorithms of midpoint displacement and Falconer algorithm).
Findings: In this work detailed methodology for surface multifractal description, which may be directly applied for data obtained from the AFM microscope, was presented.
Research limitations/implications: The geometrical features description of surfaces of the coatings obtained in the PVD and CVD processes.
Practical implications: In presented work modified PCM method for determination of the surface fractal dimension was proposed. Performed calculations proved that new method make possible to determine this parameter more correctly. Differences are especially significant for rough surfaces, as what tested using series of data sets generated by algorithms for modelling surfaces with fractional fractal dimension. Proposed modified method for determination of the fractal dimension can be used for description of the geometrical features of coatings obtained in the PVD and CVD processes.
Originality/value: Fractal and multifractal analysis gives possibility to characterise the extent of irregularities of the analysed surface in the quantitative way.
Keywords: Computer Assistance in the engineering tasks and scientific research; Fractal dimension; Multifractal spectrum

Reference to this paper should be given in the following way:
W. Kwaśny, A modification of the method for determination of surface fractal dimension and multifractal analysis, Journal of Achievements in Materials and Manufacturing Engineering 33/2 (2009) 115-125.

1. Introduction

The possibility of description of the investigated materials surfaces is an important issue for materials engineering. Such materials have characteristic geometrical features, whose description is connected with the following concepts: morphology, topography and surface shape. Investigation results [8-10] indicate existence of relationships between the coatings

surface morphology and the manufacturing technology, and determining them is very important, as the surface morphology has a significant effect on coating properties, like: roughness parameter, friction coefficient, hardness, and wear resistance [4-7]. Surface investigations of such material reveal its very important feature – irregularity, whose degree is independent on magnification used . The extent of irregularities of the analysed surface can be quantitatively characterised by the value of the surface fractal dimension D. In contrast to the integer value of the euclidean dimension (parameter used in traditional Euclidean geometry) surface fractal dimension D is the real number from the range of [2,3]. The state-of-the-art methods of the coatings surface topography description make it possible to determine relationships among the manufacturing technology parameters, structure, service properties, and their fractal dimension. Therefore, the problem of describing the geometrical features of surfaces of coatings obtained in the PVD processes is an important issue in surface engineering. A number of papers devoted to different methods of surface fractal dimension determination of engineering materials were published in recent years [11-17]. The projective covering method (PCM) is the most commonly used [6,7,18-24]. The analysed surface is divided into small fragments in that method and the areas of these fragments $A_i(\delta)$ are calculated (Fig. 1). Unfortunately, the formula which makes it possible to determine the area $A_i(\delta)$ of surfaces irregular in shape given in cited papers [6,7] was used without a mathematical proof. Moreover, the fractal dimension D values obtained with the cited formula are overstated (in same cases obtained values are larger than 3), which additionally challenges its correctness. A modification of the PCM method for determination of the surface fractal dimension is proposed in this work. Complete reasoning, leading to correct formula for determination $A_i(\delta)$ is presented. Data sets characterised by fractional fractal dimension were generated to test the modified method.

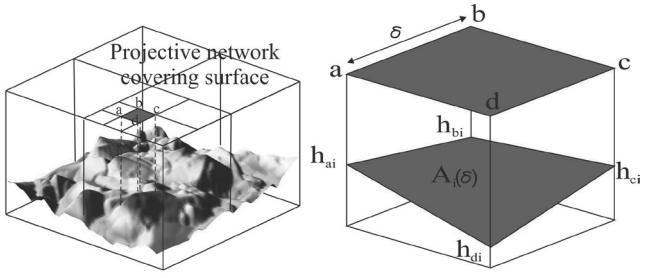

Fig. 1. Projective covering method (division of the projection plane by means of the square net along with the projection onto the analysed surface and magnification of one element of the covering projective surface along with the projection onto the part of the analysed surface)

Three different algorithms to generate data sets describing surfaces with fractional fractal dimension were used (two algorithms of midpoint displacement and Falconer algorithm). Surfaces of the investigated engineering materials generally don't exhibit a form of the purely self-similar fractals [34] and the self-similarity is local only. The surface irregularity distribution changes depending on the analysed region. Concentration of large surface irregularities occurs in some area and concentration of small irregularities are visible simultaneously in other parts. Therefore, the multifractal analysis is commonly considered as the suitable method for correct description of real surfaces [6,35,36]. The detailed methodology for surface multifractal description, which may be directly applied for data obtained from the AFM microscope, is presented in the final part of this work.

2. Algorithms for modeling surfaces with fractional fractal dimension

The trajectories of the Brownian motion represent fractal curves in 2D space, while their generalization, the so-called Brownian surfaces, form fractal surfaces in 3D space. Fractional Brownian curves/surfaces can also be defined. In the Brownian motion definition Hurst H coefficient is used. Value of H is the real number from the range of (0, 1). The classical Brownian curve (surface) is obtained for H = 1/2. Fractal dimension of the fractional Brownian motion trajectory equals 2 − H, while the fractal dimension of fractional Brownian surface equals 3 − H. All definitions and theorems (with necessary descriptions) are presented in monograph [2].

One of the Brown surface generation methods characterized by fractional dimension is the midpoint displacement method [3,4]. A square net of points is used in this algorithm (Fig. 2). During the first step heights at each corner of the analized square net are selected at random. All drawn values have to be characterised by normal distribution with zero mean and variance σ (for simplification σ = 1 can be used, such distribution will be further designated as N(0, 1)). Transformation from net of squares with sides δ (Fig. 2a) to net of squares with sides δ/2 (Fig. 4b) takes place in two stages. During the first stage heights of the centres of all squares are calculated based the heights of its four corners (Fig. 2b):

$$h_s = \frac{1}{4} \cdot (h_a + h_b + h_c + h_d) + s \cdot p \tag{1}$$

where p is a random number with normal distribution N(0, 1), and s is the scale coefficient. As a result, net of squares with sides $\delta/\sqrt{2}$ rotated of angle 45° from the initial position is obtained (Fig. 3a). In the interior part the net consists of the squares described above, at the edges it consists of triangles being halves of squares (Fig. 4a). During the second stage the heights of the centres of all squares of the rotated net are calculated (Fig. 3b). For triangles, the heights of the centres of sides on the net edge are calculated based on the heights of its three corners (Fig. 4a) :

$$h_{ts} = \frac{1}{3} \cdot (h_{ta} + h_{tb} + h_{tc}) + s \cdot p \tag{2}$$

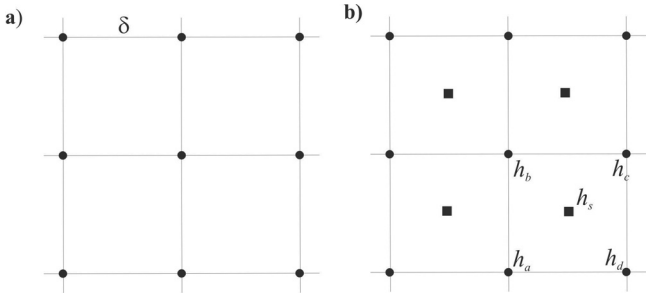

Fig. 2. Fragment of the square net at the beginning of the first step of calculations (a) and points (■), whose heights are calculated during this step (b)

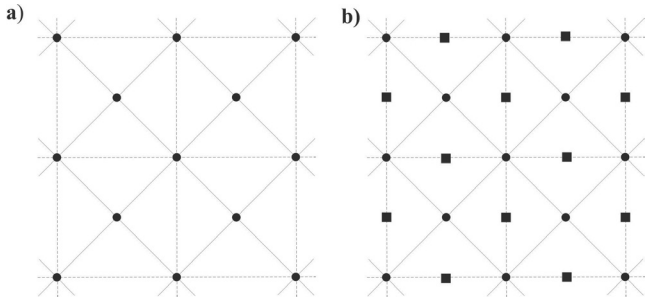

Fig. 3. Fragment of the square net at the beginning of the second step of calculations (a) and poins (■), whose heights are calculated during this step (b)

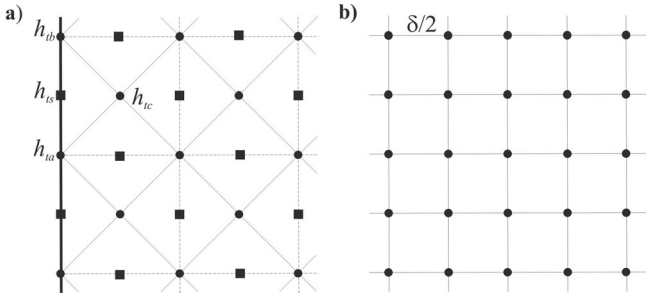

Fig. 4. Fragment of the square net next to the edge of the net (a) and fragment of the square after the second step of calculations (b)

As a result of the two steps square net with sides δ/2, oriented the same way as the initial net, is created (Fig. 4b).

Two implementations of the described algorithm are known [3,4], differing slightly from each other with the method for scale coefficient s determination. In the version proposed by Peitgen and Saupe [4] s is equal at the beginning to variance σ of the normal distribution used (usually s = 1). Before each next step of calculation its value is multiplied by $\sqrt{2^{-H}}$. In the Martyn version [3] the scale coefficient is equal to $s = \sigma\sqrt{1 - 2^{2H-2}}$ at the beginning. Next at each step, that is during transformation from square net with sides δ to square net with sides δ/2, it is multiplied by 2^{-H}.

An analytic description of the fractional Brown surface is given at work [2]:

$$W(x,y) = \sum_{k=1}^{\infty} C_k \cdot \lambda^{-k \cdot H} \cdot \sin(\lambda^k \cdot (x \cdot \cos B_k + y \cdot \sin B_k) \cdot A_k) \quad (3)$$

where H is Hurst exponent (H∈(0, 1)), λ is constant (λ>1), C_K are independent random variables with normal distribution N(0, 1), A_k and B_k are independent random variables with even distribution in range [0, 2π).

Such solution is inconvenient because it employs the infinite series. During calculations it is necessary to limit it to the finite elements only:

$$W(x,y) = \sum_{k=1}^{n} C_k \cdot \lambda^{-k \cdot H} \cdot \sin(\lambda^k \cdot (x \cdot \cos B_k + y \cdot \sin B_k) \cdot A_k) \quad (4)$$

The above-mentioned formula is a base of the third algorithm (Falconer algorithm).

Examples of fractal surfaces generated by the described algorithms for two values of Hurst exponent are presented in Figures 5-10.

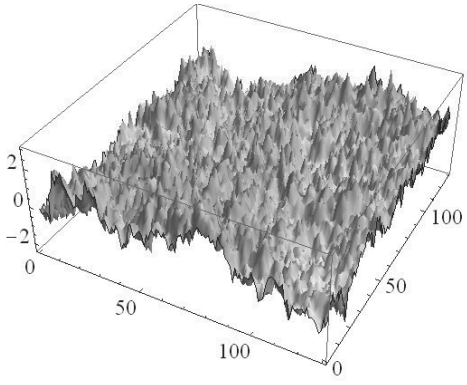

Fig. 5. Fractal surfaces generated by midpoint displacement algorithm (Peitgen and Saute version) for H = 0.25

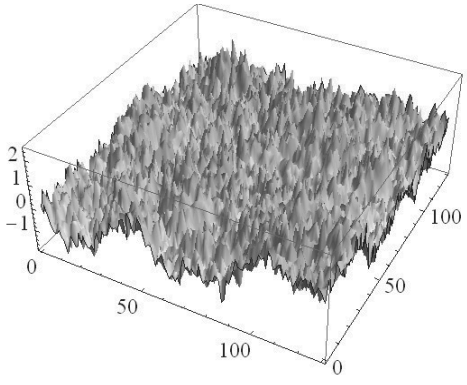

Fig. 6. Fractal surfaces generated by midpoint displacement algorithm (Martyn version) for H = 0.25

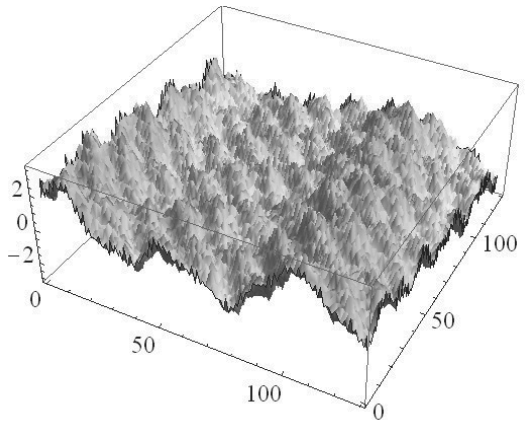

Fig. 7. Fractal surfaces generated by Falconer algorithm for H = 0.25

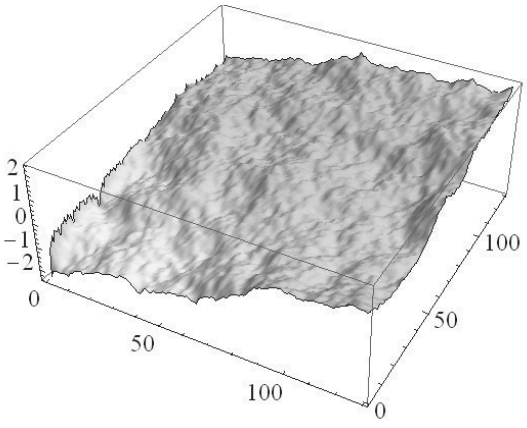

Fig. 8. Fractal surfaces generated by midpoint displacement algorithm (Peitgen and Saute version) for H = 0.75

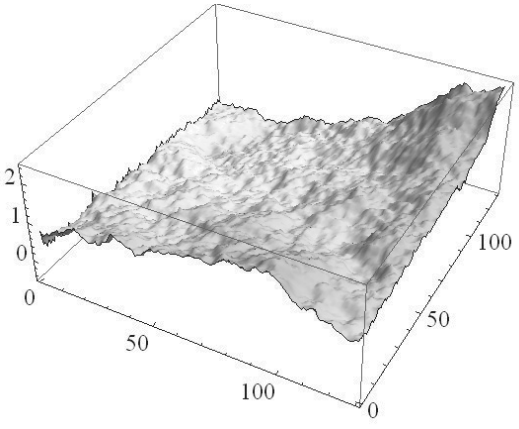

Fig. 9. Fractal surfaces generated by midpoint displacement algorithm (Martin version) for H = 0.75

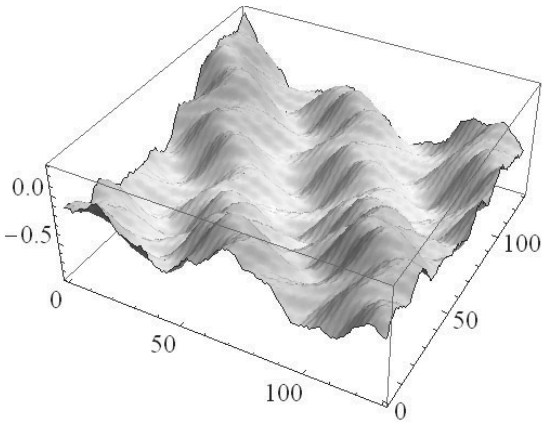

Fig. 10. Fractal surfaces generated by Falconer algorithm for H = 0.75

3. Description of the modified projective covering method for the fractal dimension determination

For any fractal set (curve, surface) the number of boxes N(δ) of side length δ required to cover considered set is described by the relationship [1,2]:

$$N(\delta) \approx \delta^{-D} \tag{5}$$

where D is the fractal dimension of the set. In order to determine the area of the fractal surface, for a fixed side length δ, the sum of the areas of the boxes covering the considered set is determined, which leads to:

$$A(\delta) = N(\delta)\,\delta^2 \tag{6}$$

Putting relationship (5) into formula (6) leads to:

$$A(\delta) \approx \delta^{2-D} \tag{7}$$

If it is possible to determine areas of the considered surfaces for chosen values of the side length δ, then the estimated value of the fractal dimension can be obtained. Exchanging the inequality (in 7) to equals sign, the following is obtained:

$$A(\delta) = C\,\delta^{2-D} \tag{8}$$

where C is the factor of proportionality. Finally, after calculations it can be expressed by:

$$\ln A(\delta) = \ln (C\,\delta^{2-D}) \tag{9}$$

and:

$$\ln A(\delta) = (2-D)\ln\delta + \ln C \tag{10}$$

In the bilogarithmic plot of (lnA(δ) versus lnδ) this relationship is linear. First, in order to determine the estimated

value of fractal dimension, points (ln δ, lnA(δ)) are calculated, at least for a few values of length δ. In an ideal case the theoretical surfaces points (lnδ, lnA(δ)) are located exactly on a straight line. This is not true in general for real surfaces. Next, the obtained data are approximated by the linear function y=α+βx. Fractal dimension is determined as:

$$D = 2 - \beta \tag{11}$$

All the above-mentioned remarks can be used only if surface A(δ) area can be calculated for the fixed side length δ. Fractal dimension does not depend on size of the surface under consideration. Making conversion of variables, it can be assumed that the analysed surface is the graph of a function h : Ω → R, where $\Omega \subset R^2$ is a square with sides parallel to the axis and equal c_0. Taking side length δ in this way that δ is a submultiple of c_0 (i.e. there exists such k∈N that $c_0 = k\,\delta$) it is possible to cover Ω with net of squares with sides parallel to axes and equal δ. Next, values of function h are determined (for real surfaces these values are known from measurements) in points indicated by this net. The analysed net consists of N(δ) squares. By determination of areas $A_i(\delta)$, i = 1, . . . ,N(δ) of all fragments of the analysed surface and by totalling them, the total area of the analysed surface can be obtained:

$$A(\delta) = \sum_{i=1}^{N(6)} A_i(\delta) \tag{12}$$

The surface area $A_i(\delta)$ described by function h over square abcd (curved set in space) in general is described by the integral:

$$P_{abcd} = \iint_{abcd} \sqrt{1 + (\frac{\partial h}{\partial x})^2 + (\frac{\partial h}{\partial y})^2}\, dxdy \tag{13}$$

The analytical formula of function h is needed, while only values of variables in four points (corners) of the square are determined during measurements. Therefore, it is necessary to specify a formula which will make it possible to estimate an area of the analysed surface using values for these points only. Using symbols like those in Figure 11, the analysed surface can be approximated by two triangles ABC and CDA. The ABC triangle surface can be determined as the area of a triangle formed with the BA and BC vectors [5]:

$$P_{ABC} = \frac{1}{2}\left|\vec{BA} \times \vec{BC}\right| = \frac{1}{2}\left|\vec{BA}\right|\left|\vec{BC}\right| \sin\varphi \tag{14}$$

where × means the cross product, || means vector length and φ is an angle between vectors BA and BC. Similarly, surface of the CDA triangle can be determined as the area of a triangle formed with the DA and DC vectors.

$$P_{CDA} = \frac{1}{2}\left|\vec{DA} \times \vec{DC}\right| \tag{15}$$

For the known vectors u = (u_x, u_y, u_z) and v = (v_x, v_y, v_z), the length of theirs cross product can be calculated as [5]:

$$\left|\vec{u} \times \vec{v}\right| = \sqrt{\begin{vmatrix} u_y & u_z \\ v_y & v_z \end{vmatrix}^2 + \begin{vmatrix} u_z & u_x \\ v_z & v_x \end{vmatrix}^2 + \begin{vmatrix} u_x & u_y \\ v_x & v_y \end{vmatrix}^2} \tag{16}$$

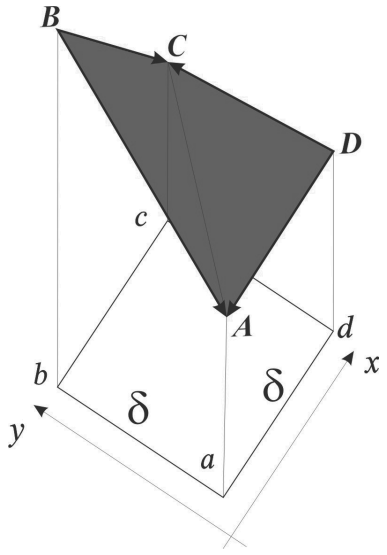

Fig. 11. Auxiliary graph for the formula for determination of the approximated value of the $A_i(\delta)$ area

Using symbols as those in Figure 11 the necessary points have coordinates:

$$A(x,y,h_{ai}),\ B(x,y+\delta,h_{bi}),\ C(x+\delta,y+\delta,h_{ci}),\ D(x+\delta,y,h_{di}) \tag{17}$$

and vectors can be calculated as:

$$\begin{aligned} \vec{BA} &= (0,-\delta,h_{ai} - h_{bi}),\\ \vec{BC} &= (\delta,0,h_{ci} - h_{bi}),\\ \vec{DA} &= (-\delta,0,h_{ai} - h_{di}),\\ \vec{DC} &= (0,\delta,h_{ci} - h_{di}). \end{aligned} \tag{18}$$

Putting formula (16) the following can be obtained:

$$\left|\vec{BA} \times \vec{BC}\right| = \delta\sqrt{\delta^2 + (h_{ai} - h_{bi})^2 + (h_{ci} - h_{bi})^2} \tag{19}$$

$$\left|\vec{DA} \times \vec{DC}\right| = \delta\sqrt{\delta^2 + (h_{ai} - h_{di})^2 + (h_{ci} - h_{di})^2} \tag{20}$$

The approximated area $A_i(\delta)$ of the analysed surface can be calculated as a sum of the ABC and CDA triangles surfaces.

$$A_i(\delta) = \frac{1}{2}\delta(\sqrt{\delta^2 + (h_{ai} - h_{bi})^2 + (h_{ci} - h_{bi})^2} + \sqrt{\delta^2 + (h_{ai} - h_{di})^2 + (h_{ci} - h_{di})^2}) \tag{21}$$

In other works [6,7] the estimated area $A_i(\delta)$ is given as:

$$A_i(\delta) = \frac{1}{2}(\sqrt{\delta^2 + (h_{ai} - h_{di})^2}\sqrt{\delta^2 + (h_{di} - h_{ci})^2} + \sqrt{\delta^2 + (h_{ai} - h_{bi})^2}\sqrt{\delta^2 + (h_{bi} - h_{ci})^2} \tag{22}$$

This formula was given without any justification. It can be justificated in the following way: the area $A_i(\delta)$ can be calculated as sum of two triangles - ABC and CDA. For these triangles the following inequalities are true:

$$P_{ABC} = \frac{1}{2}\left|\vec{BA}\times\vec{BC}\right| = \frac{1}{2}\left|\vec{BA}\right|\left|\vec{BC}\right|\sin\varphi_2 \le \frac{1}{2}\left|\vec{BA}\right|\left|\vec{BC}\right| \tag{23}$$

$$P_{ABC} = \frac{1}{2}\left|\vec{DA}\times\vec{DC}\right| = \frac{1}{2}\left|\vec{DA}\right|\left|\vec{DC}\right|\sin\varphi_2 \le \frac{1}{2}\left|\vec{DA}\right|\left|\vec{DC}\right| \tag{24}$$

where φ_1 and φ_2 are angles between vectors. Therefore, it can be assumed that the approximated area of part of analized surfaces can be calculated as sum of upper limitations of these triangles:

$$A_i(\delta) = \frac{1}{2}\left(\left|\vec{BA}\right|\left|\vec{BC}\right| + \left|\vec{DA}\right|\left|\vec{DC}\right|\right) \tag{25}$$

Then lengths of vectors have to be calculated, using formula (18), which leads to:

$$\begin{aligned}
\left|\vec{BA}\right| &= \sqrt{\delta^2 + \left(h_{ai} - h_{bi}\right)^2}, \\
\left|\vec{BC}\right| &= \sqrt{\delta^2 + \left(h_{ci} - h_{bi}\right)^2}, \\
\left|\vec{DA}\right| &= \sqrt{\delta^2 + \left(h_{ai} - h_{di}\right)^2}, \\
\left|\vec{DC}\right| &= \sqrt{\delta^2 + \left(h_{ci} - h_{di}\right)^2}.
\end{aligned} \tag{26}$$

Taking into consideration the obtained results and relationship (25), formula (22) is obtained. It means that formula given by Xie, Wang and Kwasniewski [6,7] is less universal than formula (21) because of its main additional assumption that perpendicular vectors ($\sin\varphi=1$) were used, which generally is not true.

4. Verification of the modified projective covering method for the fractal dimension determination

For verification of the modified projective covering method (with modified formula (21) for determination of value of the area $A_i(\delta)$), data sets which model surfaces with fractional fractal dimension were used. Three previously described algorithms were used for their generation: two algorithms of midpoint displacement and Falconer algorithm.

Fractal dimension results obtained for nine different Brown surfaces are presented in Tables 1-3. Results obtained for Brown surfaces generated by algorithm of random midpoint displacement (Table 1 - Peitgen and Saute version, Table 2 - Martin version) are shown in Tables 1 and 2. Results obtained for Brown surfaces generated by Falconer algorithm are presented in Table 3. In the last case only first 30 elements of the series were used (i.e. n=30) and value $\lambda = 2$ was chosen. In all surface generation cases the net of 512×512 squares was used. An area $A(\delta)$ was calculated using two formulae described earlier, for the following lengths:

$$\delta \in \{c_s, 2c_s, 4c_s, 8c_s, 16c_s, 32c_s, 64c_s, 128c_s, 256c_s, 512c_s\} \tag{27}$$

where $c_s = 1/512$ is a length of the square side in net used for simulation. As a result 10 points ($\ln\delta$, $\ln A(\delta)$) plotted on bilogarithmic graph were obtained and then approximated by linear function.

The slope of this function was used for fractal dimension determination. The relative errors calculated according following relationship are also presented in Tables:

$$E = \frac{\left|D - D_H\right|}{D_H} \tag{28}$$

where D means the calculated value of fractal dimension and $D_H = 3-H$ is the theoretical value of fractal dimension of the analysed surface.

The modified PCM method gives the fractal dimension values in range [2,3] for the three surface generation algorithms used, whereas the PCM method used so far gives senseless fractal dimension values often larger than 3, especially for surfaces with H<0.5 (Figs. 12-14). The calculations from this work prove that the modified projective covering method for the fractal dimension determination with the modified formula for determination of area of the surface irregular in shape $A_i(\delta)$ (21) gives more reasonable results (closer to the theoretical values, indicated on Figures as a straight line – optimal results) than those obtained so far using relationship (22) from work [6,7]. Differences between the old version and version proposed in this study are especially important for rough surfaces (D>2.2). These observations are also confirmed by the sum of relative errors obtained from calculations (Tables 1-3).

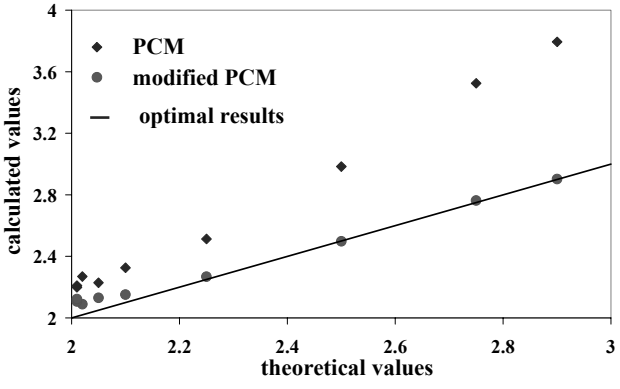

Fig. 12. Comparison of fractal dimension D obtained by PCM and modified PCM method (obtained for Brown surface generated by algorithm of random midpoint displacement - Peitgen and Saute version

Table 1.
Fractal dimension values obtained for Brown surface generated by algorithm of random midpoint displacement (Peitgen and Saute version)

Hurst coefficient H	Fractal dimension $D_H = 3\text{-}H$ (theoretical values)	Fractal dimension D (calculated values)		Relative error E	
		PCM method (relationship 22)	Modified PCM method (relationship 21)	PCM method (relationship 22)	Modified PCM method (relationship 21)
0.1	2.9	3.79367	2.90269	0.30816	0.00093
0.25	2.75	3.52401	2.76276	0.28146	0.00464
0.5	2.5	2.98363	2.49824	0.19345	0.00070
0.75	2.25	2.51345	2.26881	0.11709	0.00836
0.9	2.1	2.32628	2.15217	0.10775	0.02484
0.95	2.05	2.22865	2.13078	0.08715	0.03940
0.98	2.02	2.26917	2.08978	0.12335	0.03454
0.99	2.01	2.19915	2.10707	0.09410	0.04829
0.995	2.01	2.21061	2.12241	0.09981	0.05593

Table 2.
Fractal dimension values obtained for Brown surface generated by algorithm of random midpoint displacement (Martyn version)

Hurst coefficient H	Fractal dimension $D_H = 3\text{-}H$ (theoretical values)	Fractal dimension D (calculated values)		Relative error E	
		PCM method (relationship 22)	Modified PCM method (relationship 21)	PCM method (relationship 22)	Modified PCM method (relationship 21)
0.1	2.9	3.79417	2.89176	0.30833	0.00284
0.25	2.75	3.48295	2.74411	0.26653	0.00214
0.5	2.5	3.00181	2.50134	0.20072	0.00054
0.75	2.25	2.49395	2.25974	0.10842	0.00433
0.9	2.1	2.22727	2.12584	0.06060	0.01230
0.95	2.05	2.24844	2.09619	0.09680	0.02253
0.98	2.02	2.03660	2.02071	0.00822	0.00035
0.99	2.01	2.04201	2.02718	0.01593	0.00855
0.995	2.01	2.15584	2.01085	0.07256	0.00042

Table 3.
Fractal dimension values obtained for Brown surface generated by Falconer algorithm

Hurst coefficient H	Fractal dimension $D_H = 3\text{-}H$ (theoretical values)	Fractal dimension D (calculated values)		Relative error E	
		PCM method (relationship 22)	Modified PCM method (relationship 21)	PCM method (relationship 22)	Modified PCM method (relationship 21)
0.1	2.9	3.80302	2.90903	0.31139	0.00311
0.25	2.75	3.48020	2.75522	0.26553	0.00190
0.5	2.5	3.06106	2.56551	0.22442	0.02620
0.75	2.25	2.38910	2.24086	0.06182	0.00406
0.9	2.1	2.16977	2.08364	0.03322	0.00779
0.95	2.05	2.17457	2.12080	0.06077	0.03454
0.98	2.02	2.06241	2.04559	0.02100	0.01267
0.99	2.01	2.10795	2.07096	0.04873	0.03033
0.995	2.01	2.06442	2.04500	0.02707	0.01741

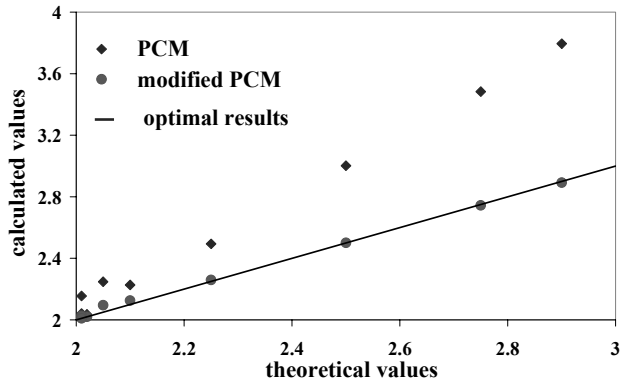

Fig. 13. Comparison of fractal dimension D obtained by PCM and modified PCM method (obtained for Brown surface generated by algorithm of random midpoint displacement - Martyn version)

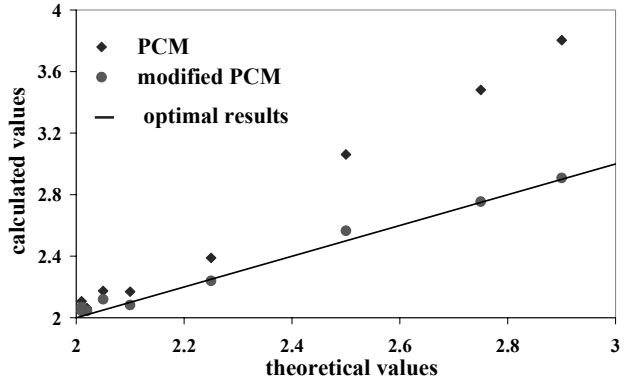

Fig. 14. Comparison of fractal dimension D obtained by PCM and modified PCM method (obtained for Brown surface generated by Falconer algorithm)

5. Methodology for surface multifractal description

The reasoning connected with the detailed methodology for surface multifractal description is based to a large degree on Xie's work [7], but some modification (modified formula (21) for determination of area of the surface irregular in shape $A_i(\delta)$) was taken into consideration. Let's consider a surface described on square (i.e. domain (the projection plane) is a square, obtained as an orthogonal projection of this set). The surface can be described by analytical function or by discrete sets (e.g. from measurements)). Covering the analysed set with the net of squares with sides δ (Fig.1) (for discrete function localization of the measurements points have to be situated at square corners), the area of a rough surface $A_i(\delta)$ connected with each fragment (square) of the projection plane can be calculated (relationship 21). By determination of areas $A_i(\delta)$, i = 1, . . . ,N(δ) of all fragments of the analysed surface and by totalling them, the total area of analized surface can be obtained (relationship 12).

The measure on each box (probability connected with each box) can be defined as :

$$P_i(\delta) = \frac{A_i(\delta)}{A(\delta)} \tag{29}$$

Parameter α_i, called Hölder exponent of singularity is also connected with each box:

$$P_i(\delta) \propto \delta^{\alpha_i} . \tag{30}$$

Let's consider $N_\alpha(\delta)$ is a number of boxes characterised by parameter α_i in range α and α+dα. Then function f(α), called multifractal spectrum, can be defined as fractal dimension of the set of boxes characterised by parameter α_i. Then:

$$N_\alpha(\delta) \approx \delta^{-f(\alpha)} . \tag{31}$$

The partial function $Z_q(\delta)$ (the so-called partition function) is defined in the following way:

$$Z_q(\delta) = \sum_{i=1}^{N(\delta)} (P_i(\delta))^q, \quad q \in R \tag{32}$$

Using this formula the generalised fractal dimension D(q) can be expressed by:

$$D(q) = \frac{1}{q-1} \lim_{\delta \to 0} \frac{\log Z_q(\delta)}{\log \delta} = \frac{1}{q-1} \lim_{\delta \to 0} \frac{\log \sum_{i=1}^{N(\delta)} (P_i(\delta))^q}{\log \delta} \tag{33}$$

For partial function $Z_q(\delta)$, the relationship is obtained [5]:

$$Z_q(\delta) \approx \delta^{q\,\alpha(q) - f(\alpha(q))} . \tag{34}$$

On putting the auxiliary function τ(q) (convex function):

$$\tau(q) = q\,\alpha(q) - f(\alpha(q)), \tag{35}$$

the previous relationship can be expressed as:

$$Z_q(\delta) \approx \delta^{\tau(q)} . \tag{36}$$

By considering the derivative of τ (q):

$$\frac{d}{dq}\tau(q) = \alpha(q) \tag{37}$$

Relationship (35) is called as Legendre transformation. From (34), (35) and (36), the relationship between auxiliary function τ (q) and generalised fractal dimension D(q) is obtained [4]:

$$\tau(q) = (q-1)D(q). \tag{38}$$

The normalized measure is construed on probability values in such a way that for each q value measure (probability) connected with box indexed by "i" is defined as [1, 2]:

$$\mu_i(q,\delta) = \frac{(P_i(\delta))^q}{\sum_{i=1}^{N(\delta)}(P_i(\delta))^q} = \frac{(P_i(\delta))^q}{Z_q(\delta)} \tag{39}$$

It can be obtained from (38) and (33):

$$\tau(q) = \lim_{\delta\to 0}\frac{\log Z_q(\delta)}{\log(\delta)} = \lim_{\delta\to 0}\frac{\log\sum_{i=1}^{N(\delta)}(P_i(\delta))^q}{\log\delta} \tag{40}$$

On putting (37) and defined above measure the following relationship is true:

$$\alpha(q) = \lim_{\delta\to 0}\frac{\sum_{i=1}^{N(\delta)}(\mu_i(q,\delta)\log P_i(\delta))}{\log\delta}, \tag{41}$$

Similar relationship can be obtained for the multifractal spectrum f(α) [1]:

$$f(q) = \lim_{\delta\to 0}\frac{\sum_{i=1}^{N(\delta)}(\mu_i(q,\delta)\log\mu_i(q,\delta))}{\log\delta} \tag{42}$$

Relationship (33) makes it possible to determine the generalised fractal dimension for q ≠ 1. On putting $D(1) = \lim_{q\to 1} D(q)$ we get:

$$D(1) = \alpha(1) = f(\alpha(1)). \tag{43}$$

On employing relationships described above two algorithms for multifractal spectrum f(α) and the generalised fractal dimension calculation can be produced. There are the moments method algorithm [5] and Chabry-Jensen algorithm [2, 1] (see also [7, 8]).

5.1. Moments method algorithm

1. Exponent values q_k, k = 1, 2, . . . , n_q, and length of the box sides δ_j, j = 1, 2, . . . , n_δ are fixed
2. The projection plane is covered by boxes with side lengths δ_j, for j = 1, 2, . . . , n_δ, and then value $P_i(\delta_j)$ is determined for each box measure (relationship (29)).
3. The partial function $Z_q(\delta)$ values for fixed δ_j and q_k are determined (relationship (32)).
4. For q_k, k = 1, 2, . . . , n_q, relationships between log $Z_{qk}(\delta_j)$ and log δ are tested. If such relationships are linear, than $\tau(q_k)$ is equal the slope of the line (relationship 36).
5. On employing Legendre transformation values of $\alpha(q_k)$ and $f(\alpha(q_k))$ are computed.
6. The generalised fractal dimension $D(q_k)$ can be easily calculated using $\tau(q_k)$ values obtained earlier (point 4) in formula (38), with $q_k = 1$ and $D(1) = \alpha(1)$ (relationship (43)).

5.2. A Chabra-Jensen algorithm

1. 1.Exponent values q_k, k = 1, 2, . . . , n_q, and length of the box sides δ_j, j = 1, 2, . . . , n_δ are fixed.
2. The projection plane is covered by boxes with side lengths δ_j, for j = 1, 2, . . . , n_δ, and then value $P_i(\delta_j)$ is determined for each box measure (relationship (29)).
3. For each box and for fixed values δ_j and q_k values of the normalized measure $\mu_i(q_k, \delta_j)$ are determined (relationship (39)).
4. For fixed values of q_k values of Hölder exponent of singularity are determined as the slope of the approximation line for relationship:

$$\sum_{i=1}^{N(\delta)}(u_i(q_k,\delta)\log(P_i(\delta)) \tag{44}$$

which is a consequence of (41).

5. Values of the multifractal spectrum $f(q_k)$, for fixed q_k, are determined as the slope of the approximation line for relationship:

$$\sum_{i=1}^{N(\delta)}(u_i(q_k,\delta)\log u_i(q_k,\delta)) \tag{45}$$

which is a consequence of (41).

6. Values of the generalised fractal dimension $D(q_k)$, for fixed q_k, $q_k \neq 1$, can be determined as division of slope value of the approximation line for relationship:

$$\log\sum_{i=1}^{N(\delta)}(P_i(\delta))^{q_k} \tag{46}$$

and binomial q − 1 (which is a consequence of (33)). For dla $q_k = 1$ we give $D(1) = \alpha(1)$ (relationship (43)).

A typical example of the multifractal spectrum is presented in Figure 15. Two parameters (width Δα and the spectrum arms' heights difference Δf) are two most important characteristics in the description in the multifractal [11]. Width of the multifractal spectrum Δα is determined as:

$$\Delta\alpha = \alpha_{\max} - \alpha_{\min}, \tag{47}$$

while the spectrum arms' heights difference Δf is defined as:

$$\Delta f = f(\alpha_{\min}) - f(\alpha_{\max}). \tag{48}$$

Results of the multifractal analysis of the surface topography obtained from the AFM microscope described in the literature [40] suggest that the spectrum breadth is connected with roughness of coatings. Parameters $f(\alpha_{max})$ and $f(\alpha_{min})$ reflect the numbers of boxes ($N_{Pmax}(\delta)=N_{\alpha min}\sim\delta^{-f(\alpha min)}$) with the maximum and ($N_{Pmin}(\delta)=N_{\alpha max}\sim\delta^{-f(\alpha max)}$) minimum probability values respectively. Value $\Delta f=f(\alpha_{min})- f(\alpha_{max})$ is a measure of the ratio of the number of boxes with the highest probability to the number of boxes with the lowest probability ($N_{Pmax}(\delta)/N_{Pmin}(\delta)=\delta^{-\Delta f}$). In case of $\Delta f>0$ the fragments described by the high probability value predominate; whereas, in case of $\Delta f<0$ the fragments described by the low probability value predominate. Interpretation of the width of arm's spacing of the multifractal spectrum has been also provided in papers [41-44]:

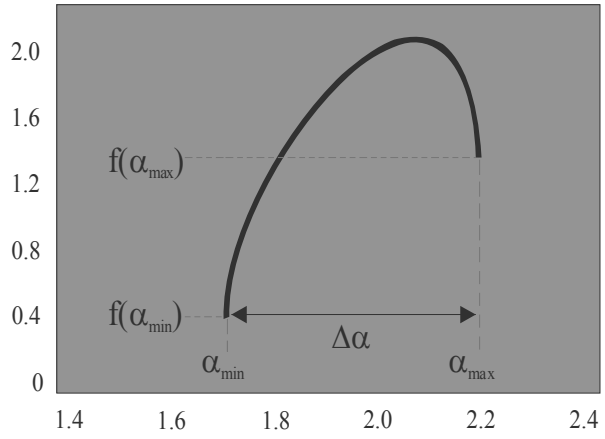

Fig. 15. Example of the multifractal spectrum

6. Conclusions

The modified PCM method for determination of the surface fractal dimension was proposed in the presented work. Calculations performed proved that the new method makes it possible to determine this parameter more correctly. Differences are especially significant for rough surfaces, as was tested using series of data sets generated by algorithms for modelling surfaces with fractional fractal dimension. The proposed modified method for determination of the surface fractal dimension can be used for description of the geometrical features of coatings obtained in the PVD and CVD processes, which was implied by the author in his earlier works [25-33], where the described modification was not taken into consideration.

Acknowledgements

Investigations were financed in part within the Rector's habilitation grant BW/RGH-12/RMT-0/2009 framework headed by PhD. W. Kwaśny.

References

[1] M.F. Barnsley, Fractals Everywhere, Academic Press, Boston, 1993.
[2] K. Falconer, Fractal Geometry. Mathematical Foundations and Applications, Wiley, Chichester, 2003.
[3] T. Martyn, Fractal and algorithm object, Nakom, Poznan, 1996 (in Polish).
[4] H.O. Peitgen, D. Saupe (eds.), The Sciences of Fractal Images, Springer-Verlag, New York, 1988.
[5] Engineering guide-book, Mathematics, vol. I and II, WNT, Warsaw, 1987.
[6] H. Xie, J.A. Wang, E. Stein, Direct Fractal Measurement and Multifractal Properties of Fracture Surfaces, Physics Letters A 242 (1998) 41-50.
[7] H. Xie, J.A. Wang, M.A. Kwaśniewski, Multifractal characterization of rock fracture surfaces, International Journal of Rock Mechanics and Mining Sciences 36 (1999) 19-27.
[8] W. Kwaśny, L.A. Dobrzański, S. Bugliosi, Ti+TiN, Ti+Ti(C_xN_{1-x}), Ti+TiC PVD coatings on the ASP 30 sintered high-speed steel, Journal of Materials Processing Technology 157-158 (2004) 370-379.
[9] L.A. Dobrzański, W. Kwaśny, Z. Brytan, R. Shishkov, B. Tomov, Structure and properties of the Ti + Ti(C,N) coatings obtained in the PVD process on sintered high speed steel, Journal of Materials Processing Technology 157-158 (2004) 312-316.
[10] K. Gołombek, L.A. Dobrzański, M. Soković, J. Kopač, Functional properties of cemented carbides with PVD and CVD wear resistant coatings, Mechanic 4 (2005) 321-327 (in Polish).
[11] A.J. Perry, The surface smoothing of TiN coatings deposited by CVD or PVD methods, Surface and Coatings Technology 132 (2000) 21-31.
[12] A. Provata, P. Falaras, A. Xagas, Fractal features of titanium oxide surfaces, Chemical Physic Letters 297 (1998) 484-490.
[13] E. Charkaluk, M. Bigerelle, A. Iost, Fractals and fracture, Engineering Fracture Mechanics 61 (1998) 119-139.
[14] L. Czarnecki, A. Garbacz, J. Kurach, On the characterization of polymer concrete fracture surface, Cement and Concrete Composites 23 (2001) 399-409.
[15] C. Atzeni, G. Pia, U. Sanna, N. Spanu, A fractal model of the porous microstructure of earth-based materials, Construction and Building Materials 22 (2008) 1607-1613.
[16] C. Dominkovics, G. Harsányi, Fractal description of dendrite growth during electrochemical migration, Microelectronics Reliability 48 (2008) 1628-1634.
[17] T. Ficner, Fractal strength of cement gels and universal dimension of fracture surfaces, Theoretical and Applied Fracture Mechanics 50 (2008) 167-171.
[18] W. Yili, D. Baiyu, L. Jie, L. Jia, S. Baoyou, T. Hongxiao, Surface analysis of cryofixation-vacuum-freeze-dried polyaluminum chloride–humic acid (PACl–HA) floks, Journal of Colloid and Interface Science 316/2 (2007) 457-466.
[19] Y. Jiang, B. Li, Y. Tanabashi, Estimating the relation between surface roughness and mechanical properties of rock joint, International Journal of Rock Mechanics and Mining Sciences 43/6 (2006) 837-846.

[20] H.W. Zhou, H. Xie, Direct Estimation of the Fractal Dimensions of a Fracture Surface of Rock, Surface Review and Letters 10/5 (2003) 751-762.
[21] A. Yan, K.R. Wu, Z. Dong, Y. Wu, Influence of concrete composition on the characterization of fracture surface, Cement and Concrete Composites 25/1 (2003) 153-157.
[22] Z.Y. Yang, C.C. Di, A directional method for directly calculating the fractal parameters of joint surface roughness, International Journal of Rock Mechanics and Mining Sciences 38/8 (2001) 1201-1210.
[23] H. Song, L. Min, X. Jun, S. Lushi, L. Peisheng, S. Sheng, S. Xuexin, Fractal characteristic of three Chinese coals, Fuel 83/10 (2004) 1307-1313.
[24] Y. Ju, S. Sudak, H. Xie, Study on stress wave propagation in fractured rocks with fractal joint surfaces, International Journal of Solids and Structures 44/13 (2007) 4256-4271.
[25] W. Kwaśny, L.A. Dobrzański, Deposition conditions effect on physical properties and surface topography fractal dimension of the Ti+Ti(C_xN_{1-x}) coatings obtained in the PVD process, Materials Engineering 3/140 (2004) 607-610.
[26] W. Kwaśny, L.A. Dobrzański, M. Pawlyta, W. Gulbiński, Fractal nature of surface topography and physical properties of the coatings obtained using magnetron sputtering, Journal of Materials Processing Technology 157-158 (2004) 183-187.
[27] W. Kwaśny, L.A. Dobrzański, Deposition conditions effect on physical properties and surface topography fractal dimension of the TiN, Ti+Ti(C,N) and TiC coatings obtained in the PVD process, Mechanic 4 (2005) 328-332 (in Polish).
[28] W. Kwaśny, L.A. Dobrzański, Structure, physical properties and fractal character of surface topography of the Ti+TiC coatings on sintered high speed steel, Journal of Materials Processing Technology 164-165 (2005) 1519-1523.
[29] W. Kwaśny, L.A. Dobrzański, Structure, physical properties and fractal character of surface topography of the Ti+TiC coatings on sintered high speed steel, Proceedings of the 13th International Scientific Conference „Achievements in Mechanical and Materials Engineering" AMME'2005, Gliwice–Wisła, 2005, 387-390.
[30] W. Kwaśny, L.A. Dobrzański, Deposition conditions effect on physical properties and surface topography fractal dimension of the PVD coatings obtained on sintered high speed steel, Proceedings of the 3rd Scientific Conference "Materials, Mechanical and Manufacturing Engineering" M^{3}E'2005, Gliwice–Wisła, 2005, 151-158 (in Polish).
[31] W. Kwaśny, J. Mikuła, L.A. Dobrzański, Fractal and multifractal characteristics of coatings deposited on pure oxide ceramics, Journal of Achievements in Materials and Manufacturing Engineering 17 (2006) 257-260.
[32] W. Kwaśny, D. Pakuła, M. Woźniak, L.A. Dobrzański, Fractal and multifractal characteristics of CVD coatings deposited onto the nitride tool ceramics, Journal of Achievements in Materials and Manufacturing Engineering 20 (2007) 371-374.
[33] W. Kwaśny, M. Woźniak, J. Mikuła, L.A. Dobrzański, Structure, physical properties and multifractal characteristics of the PVD and CVD coatings deposition onto the Al_2O_3+TiC ceramics, Journal of Computational Materials Sciences and Surface Engineering 1/1 (2007) 97-113.
[34] A.B. Chhabra, R.V. Jensen, Direct determination of the f(α) singularity spectrum, Physical Review Letters 62 (1989) 1327-1330.
[35] S. Stach, J. Cybo, J. Chmiela, Fracture surface fractal or multifractal?, Materials Characterization 46/2-3 (2001) 163-167.
[36] N.E. Odling, Natural fracture profiles, fractal dimension and joint roughness coefficients, Rock Mechanics and Rock Engineering 27 (1994) 135-153.
[37] A.B. Chabra, Ch. Meneveau, R.V. Jensen, K.R. Sreenivasan, Direct determination of the f(α) singularity spectrum and its application to fully developed turbulence, Physical Review A 40 (1989) 5284-5294.
[38] E. Ott, Chaos in Dynamical Systems, Cambridge University Press, Cambridge, 1993.
[39] H.O. Peitgen, H. Jürgens, D. Saupe, Chaos and Fractals. New Frontiers of Science, Springer-Verlag, New York, 1992.
[40] H.-S. Yu, X. Sun, S.-F. Luoa, Y.-R. Wang, Z.-Q. Wu, Multifractal spectra of atomic force microscope images of amorphous electroless Ni–Cu–P alloy, Applied Surface Science 191/1-4 (2002) 123-127.
[41] S. Stach, J. Cwajna, S. Roskosz, J. Cybo, Multifractal description of fracture morphology: Quasi 3D analysis of fracture surfaces, Materials Science 23 (2005) 573-581.
[42] S. Stach, J. Cybo, Multifractal description of fracture morphology: Theoretical basis, Materials Characterization 51 (2003) 79-85.
[43] S. Stach, S. Roskosz, J. Cybo, J. Cwajna, Multifractal description of fracture morphology: Investigation of the fractures of sintered carbides, Materials Characterization 51 (2003) 87-93.
[44] S. Stach, M. Sozańska, J. Cybo, J. Cwajna, Evaluation of the share of overlaps 34CrMo4 steel fractures by surface stereometry method and multifractal analysis, Acta Metallurgica Slovaca 10 (2004) 768-770.